ELSEVIER

Journal of Hydrology 240 (2001) 206–224

Journal of Hydrology

www.elsevier.com/locate/jhydrol

A model of the early evolution of karst aquifers in limestone in the dimensions of length and depth

F. Gabrovšek[a,b], W. Dreybrodt[b,*]

[a]*Institute of Experimental Physics, University of Bremen, P.O. Box 330 440, D-28334 Bremen, Germany*
[b]*Karst Research Institute, ZRC SAZU, Postojna, Slovenia*

Received 2 November 1999; revised 21 July 2000; accepted 21 August 2000

Abstract

A new model of the early evolution of limestone karst aquifers in the dimensions of length and depth is presented. In its initial state the aquifer consists of a rock massive with evenly spaced fractures of about 50 μm aperture widths with an hydraulic conductivity of 10^{-7} ms^{-1}. In addition to this a coarser network of prominent fractures with aperture widths of several 100 μm is also present. Boundary conditions of constant recharge 450 mm/year, or constant head from the input of allogenic streams are imposed. First the position of the water table in the aquifer is calculated, then dissolutional widening during a time step in all the fractures below the water table is found by use of the well-known nonlinear dissolution kinetics of limestone. This is iterated and the position of the water table as well as the fracture widths are found as a function of time. In the case of constant recharge to a karst plateau, the water table in any case drops to base level and conduits there propagate from the spring headwards. If constant head conditions are valid the position of the water table remains almost stable and conduits propagate along the water table from the input towards the spring. There is competition between conduit evolution along prominent fractures and along tight fissures close to the water table. In any case under constant head conditions one of these pathways wins, and early karst evolution is terminated by a breakthrough event with an explosive increase of the flow through the aquifer until constant head conditions break down. Depending on the boundary conditions of constant head or constant recharge or a combination of both it is possible to describe models of cave genesis, which have been derived from field evidence, such as the water table models of Swinnerton (Geol. Soc. Am. Bull., 34 (1932) 662) and Rhoades and Sinacori (J. Geol., 49 (1941) 785) as well as the four-state model by Ford and Ewers (Can. J. Earth Sci., 15 (1978) 1783).

Keywords: Karst aquifer; Limestone dissolution; Dissolution rates; Cave genesis; Hydraulic conductivity

1. Introduction

A mature karst aquifer shows an extremely heterogeneous spatial distribution of hydraulic conductivities in the range from 10^{-10} up to 10^{-1} ms^{-1}. The low conductivities relate to the rock matrix (10^{-10} ms^{-1}), and the highest ones to large conduits draining the system ($>10^{-1}$ ms^{-1}) (Worthington, 1999; Worthington and Ford, 1997). Consequently a mature karst landscape is characterized by the absence of surface flow. The water table underground, separates the zones of vadose and phreatic flow. The evolution of an initially relatively homogenous rock, characterized by the rock matrix and primary fractures with widths of less than 10^{-2} cm to a heterogeneous karst aquifer is driven by dissolutional widening of the primary

* Corresponding author. Fax: +49-421-218-7318.
E-mail address: dreybrod@physik.uni-bremen.de (W. Dreybrodt).

0022-1694/01/$ - see front matter
PII: S0022-1694(00)00323-1

fractures, such as joints and bedding plane partings, by calcite aggressive $H_2O–CO_2$ solutions infiltrating from the surface (Dreybrodt, 1988; Ford and Williams, 1989; White, 1988). As a result cave conduits form mainly along these fractures. Palmer (1991) concluded that about 60% of all conduits follow bedding planes, and 40% are oriented along joints. But also other narrow fractures are enlarged, such that the average conductivity in those areas without conduits increases from about 10^{-7} to about 10^{-5} ms^{-1} in well-karstified regions (Sauter, 1991).

In the last decade a series of attempts have been taken to understand the evolution of such complex aquifers by computer models (Dreybrodt, 1988, 1990, 1996; Dreybrodt and Siemers, 2000; Groves and Howard, 1994a,b; Howard and Groves, 1995; Clemens et al., 1996, 1997, 1999; Siemers and Dreybrodt, 1998; Kaufmann and Braun, 1999, 2000; Lauritzen et al., 1992; Palmer 1984, 1991, 2000; Hanna and Rajaram, 1998; Gabrovšek and Dreybrodt, 2000a,b; Ford et al., 2000). An indispensable ingredient to all models is a firm knowledge on the dissolution rates of limestone, from which widening of the fractures can be calculated. These rate laws have been experimentally found as

$$F(c) = k_1(1 - c/c_{eq}) \text{ for } c < c_s$$
$$F(c) = k_n(1 - c/c_{eq})^n \text{ for } c \geq c_s \quad (1)$$

where k_1 and k_n are rate constants in mol/(cm^2 s); c the concentration of Ca^{2+} ions in mol/cm^3; and c_{eq} the equilibrium concentration with respect to calcite; c_s a switch concentration, where the kinetics switches from a linear rate law to a nonlinear rate law, with n between 3 and 10 (Eisenlohr et al., 1999; Svensson and Dreybrodt, 1992; Palmer, 1991, 1984; Buhmann and Dreybrodt, 1985; Dreybrodt et al., 1996; Dreybrodt and Eisenlohr, 2000; Plummer and Wigley, 1976)

It has turned out that this nonlinear behavior of the rates close to equilibrium is essential to the origin of karst conduits. If the dissolution rate laws were entirely linear ($c_s = c_{eq}$), water penetrating into fissures would attain equilibrium after penetration of only a few meters into the rock because the dissolution rates drop exponentially. In contrast, nonlinear kinetics allows deep penetration into the rock, such that even after distances of kilometers a small, but sufficient solutional power exists, which can create conduits (Dreybrodt and Gabrovšek, 2000).

Geological settings in the formation of karst aquifers are complex and therefore different approaches in modeling the evolution of karst aquifers have been taken. The early models presented by Dreybrodt (1990) and Palmer (1991), and those by Groves and Howard (1994a) assumed constant head conditions between inflow and outflow of the initial karst aquifer. They further assumed that flow through the aquifer propagates along initially narrow fractures of several 10^{-2} cm aperture widths and neglected entirely flow through tight fissures. As long as such conditions persist, a positive feedback loop is active since increase in the fracture widths causes accelerated dissolution and vice versa. Therefore after an initially slow increase, a dramatic explosion of flow rates and of fracture widening results. This event, termed as breakthrough terminates the early evolution of a karst aquifer. It has been shown (Dreybrodt, 1996; Siemers and Dreybrodt, 1998; Gabrovšek and Dreybrodt, 2000a) that the time required for this to happen can be approximated by an analytic expression, which specifies all parameters, which determine karstification. Further evolution of the aquifer after breakthrough is controlled by recharge through the aquifer and has been modeled by Kaufmann and Braun (2000) assuming phreatic conditions in the entire aquifer.

A different approach has been taken by Clemens et al. (1996, 1997,1999). These authors used a single-continuum discrete-network model (Sauter, 1991, 1993; Teutsch and Sauter, 1991). This approach is based upon hydraulic coupling of a pipe network representing larger prominent fractures, to a continuum, which represents a system of narrow fissures. Dissolutional widening is taken into account only in the system of pipes but not in the continuum of small fissures. The enlarging conduits drain this continuum. Therefore flow through these increases and a conduit system originates. In this approach constant recharge to the aquifer controls the hydraulic heads. As the conduit system enlarges the heads in the continuum drop and flow is attracted by the conduits. This model needs, as an important parameter, an exchange coefficient, which couples the pipe system and the continuum. This parameter, however, is not easy to access. Therefore Kaufmann and Braun (2000) have

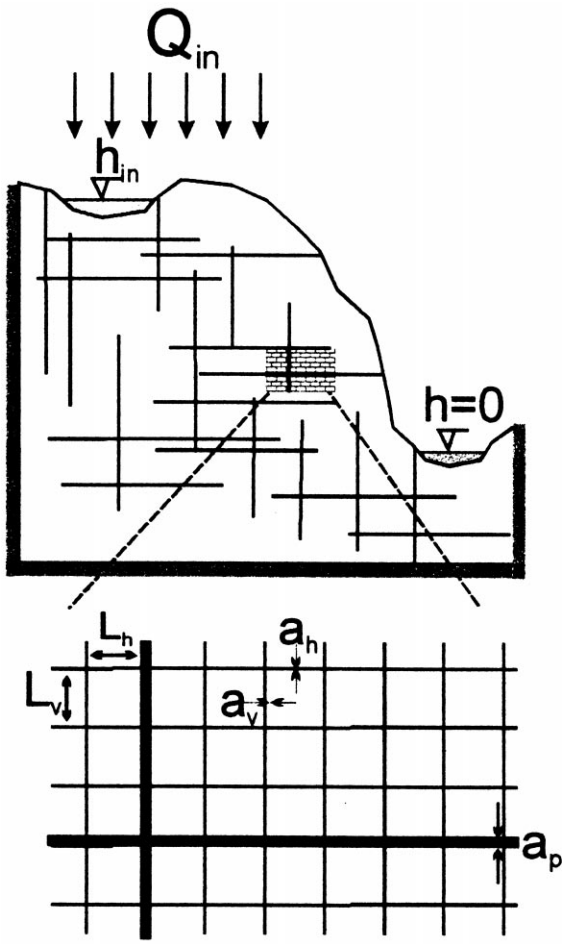

Fig. 1. Conceptual model of a karst aquifer in its initial state. Q_{in} indicates annual precipitation. At the upper left top a lake delivers input at constant head h_{in}. Baselevel is represented by a river at $h = 0$. The fractures indicated in the upper figure are wide, prominent fractures, imbedded into a net of fine fractures, with widths a_v and a_h, respectively (lower pannel). Grid size $L_h = 2$ m and $L_v = 0.5$ m is used later on.

used a discrete fracture approach which incorporates the prominent fractures directly into the medium of the continuum to avoid this exchange parameter. Their results, however, are similar.

All models presented so far are incomplete. Either they neglect the continuum completely, or at least they neglect dissolutional widening of the many fissures comprising it. By that way they may be regarded as end members of a more comprehensive model. The approach of maintaining constant head and neglecting fissures with small aperture widths may be more appropriate to describe early karstification in confined aquifers, whereas the single-continuum discrete-network models have their merits describing an intermediate phase of aquifer evolution, when the conductivity of the continuum has increased such that it can be no longer neglected. At that time the continuum can drain a sufficient amount of flow and the constant head condition breaks down.

In between these two stages of aquifer development, conditions should exist where increasing conductivity of the continuum provides a further interaction mechanism between the prominent fractures and the continuum. On the other hand, if the fissures are evenly distributed and no prominent fractures are present, it should be possible to model the evolution of such a network. In this work we present such approaches to a more realistic understanding of karst evolution.

2. Modeling concepts

Fig. 1 presents the basic concept of the karst system at the beginning of its evolution. A limestone plateau with a vertical cliff is dissected by horizontal and vertical fractures. The prominent fractures with large aperture widths a_p are shown in the upper part of the figure. The magnification in its lower part illustrates the continuum of narrow horizontal and vertical fissures with even spacings L_h, L_v and aperture widths a_h and a_v, respectively ($L_v = 50$ cm, $L_h = 200$ cm, $a_v \approx a_h \approx 5 \times 10^{-3}$ cm, $a_p \approx 2 \times 10^{-2}$ cm). This setting is idealized by a rectangular net with dimension 100×60 representing 200 m horizontal and 30 m vertical extension. Thus grids with 2 m horizontal and 0.5 m vertical spacings are used. To each set of fractures a hydraulic conductivity k can be assigned by

$$k = \frac{\rho g a^3}{12 \mu s} \tag{2}$$

where g is earth gravitational acceleration; μ the viscosity of water, and ρ its density, a the aperture width and s the spacing between the fractures (Lee and Farmer, 1993). For $a = 5 \times 10^{-3}$ cm and $s = 100$ cm this corresponds to a value of $k = 10^{-7}$ ms^{-1}, which is characteristic to nonkarstified limestone. The left-hand side, the lower boundary

and the lower part of the right-hand site boundary are assumed as impermeable as indicated in the figure. The head fixed at the river is zero. A recharge of 450 mm/year is evenly distributed to the aquifer. Additionally constant head conditions can be employed to simulate a river flowing on the plateau of the karst area.

The evolution of the aquifer is found iteratively using the following procedure:

1. An initial guess for the water table is chosen and the constant recharge Q is evenly distributed to all its nodes. At the locations of constant head this is applied to the entrance of the corresponding fractures. At the permeable right-hand side the head applied to each fracture is equal to its elevation, such that seepage flow occurs from the fractures. The initial guess for the water table at time zero is the top of the aquifer. At later time steps the water table existing one time step back is chosen as initial guess.
2. The hydraulic heads at all the points in the entire net of the assumed water table are calculated as reported by Siemers and Dreybrodt (1998). Points above the assumed water table are omitted from the calculation. To solve the equations for the heads we used the method of sparse matrix implementation of the preconditioned conjugate gradient method (Meschach matrix library in C).
3. Each node on this water table is checked for the water table condition, i.e. the hydraulic head has to be equal to its height. (a) If nodes at the upper surface of the aquifer exhibit hydraulic heads larger than their elevation, the hydraulic head is set equal to the elevation. (b) If the head of a node inside the aquifer is higher than its height, the position of the water table is shifted up by one node, if it is lower, it is shifted down to the node below. No problems with convergence did occur in this iterative procedure. When we tried to use larger grid distances to simulate larger aquifers, certain nodes were found to be below the water table in one iteration and above in the next, such that no convergence was obtained. Therefore our computer runs were restricted to the grid size and the dimensions of the aquifer, as reported here. More sophisticated programs will be worked out by our group in the future. (see also Section 4).
4. Steps 2 and 3 are iterated until all the points at the assumed water table fulfill the water table condition.
5. Once the position of the water table is known, the heads at all nodes in the aquifer are calculated. From this the flow through each fracture is found. Then the dissolution procedure reported by Siemers and Dreybrodt (1998) is used to calculate dissolutional widening in all fractures during a given time interval. The time intervals (between 10 and 50 years) are chosen so that further reduction does not affect the results. Laminar flow was verified at the end of each time step by determining the Reynolds number in each fracture to be 1000.
6. Steps 1–5 are iterated to find the position of the water table and the widths of all fractures as they change in time.

A list of all parameters used is given by Table 1.

3. Results

3.1. Initially homogenous aquifers: conditions of constant recharge

Fig. 2 represents the evolution of an aquifer with evenly spaced narrow fissures ($a_v = 6 \times 10^{-3}$ cm, $a_h = 7 \times 10^{-3}$ cm) and no prominent fractures present. The parameters used to obtain dissolution widening are $k_1 = 4 \times 10^{-11}$ mol/(cm^2 s), $n = 4$,

Table 1
List of symbols

Description	Name	Unit
Aperture width of horizontal and vertical fissures	a_h,a_v	cm
Aperture width of prominent fractures	a_p	cm
Length of vertical and horizontal fractures	L_v, L_h	cm
Spacing between the fractures	s	cm
Hydraulic head	h	cm
Hydraulic conductivity	k	ms^{-1}
Annual recharge	Q	mm/year
Order of nonlinear kinetics	n	
Nonlinear kinetics constant	k_n	mol/cm^{2}s
Concentration of calcium	c	mol/cm^3
Switch concentration	c_s	mol/cm^3
Equilibrium concentration	c_{eq}	mol/cm^3
Viscosity of the solution	μ	g/cm s
Density of the solution	ρ	g/cm^3

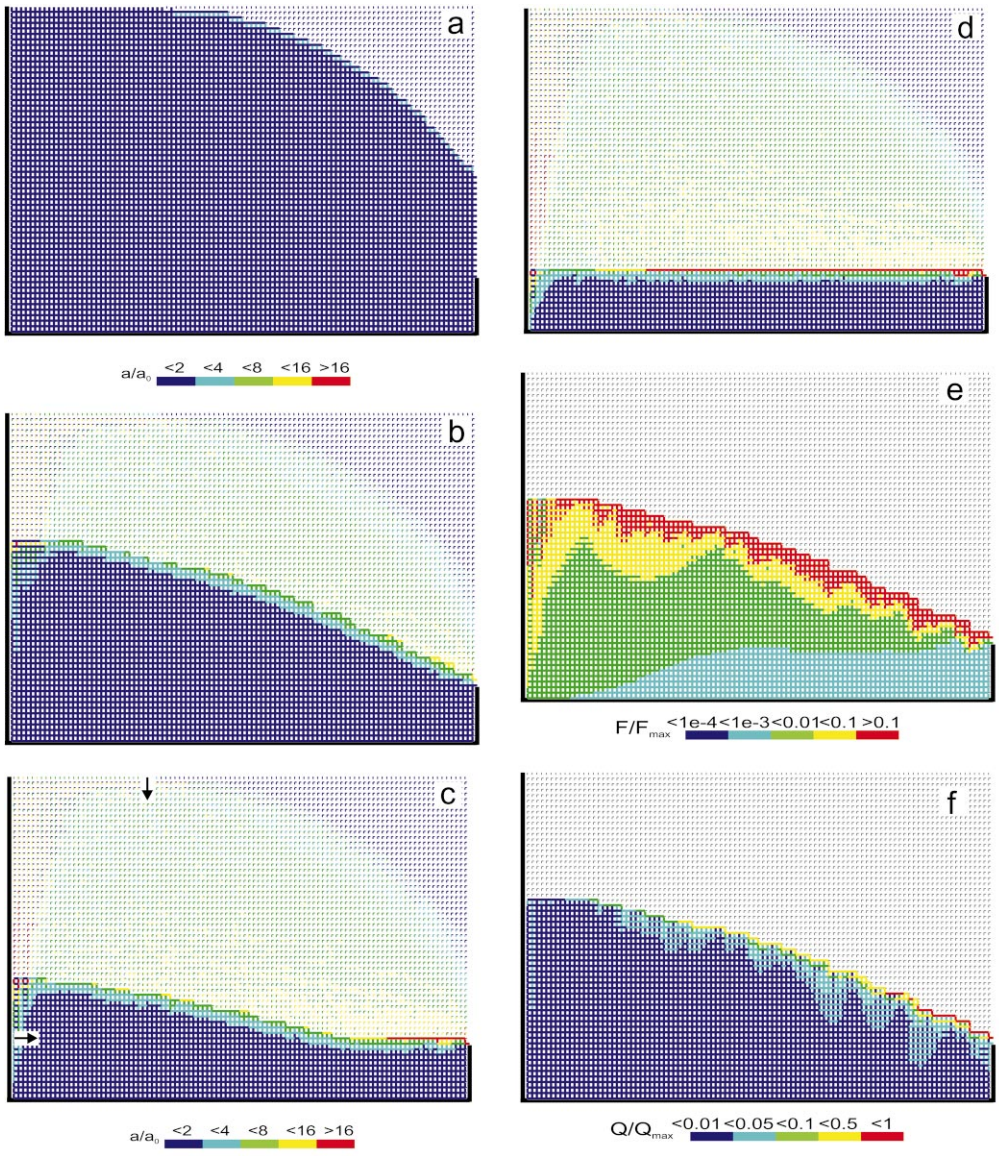

Fig. 2. Evolution of an aquifer with evenly spaced fractures and constant recharge. Distribution of fracture widths in the initial state after (a) 50, (b) 5000, (c) 10 000 and (d) 15 000 years. The colors represent the widths of the fractures in units $a(t)/a_0$, where a_0 is the initial width of vertical fractures ($a_0 = a_v(t = 0)$). Fractures designated by full squares represent the phreatic zone, those by open angels the vadose zone. The water table is thus clearly presented. The initial state is shown by (a), which also depicts a narrow fringe of vertical fractures already widened after only 50 years. The water table drops continuously leaving increased fracture widths (hydraulic conductivity) in the vadose zone, and a fringe of increased conductivity on the top of the phreatic zone (b). After 10 000 years (c) the water table has dropped to base level, where a conduit (red) with an exit width of 0.2 cm starts to grow headwards. It has propagated further after 15 000 years (d). Its exit width is now 0.6 cm. Compare also Fig. 3. Note that the phreatic zone below the fringe of increased widths exhibits low conductivity at all times since virtually no dissolutional widening is active in this region. (e) Dissolution rates in units F/F_{max} where $F_{max} = 4 \times 10^{-12}$ mol/(cm^2 s) corresponding to bedrock retreat of few 10^{-3} cm/year. The maximal dissolution is active close to the water table and drops rapidly with depth. (f) Flow rates in units of Q/Q_{max} at 5000 years. The fracture with the highest flow rate has Q/Q_{max} close to 1. Most of the flow is concentrated to the permeable fringe at the top of the phreatic zone. Confer (b).

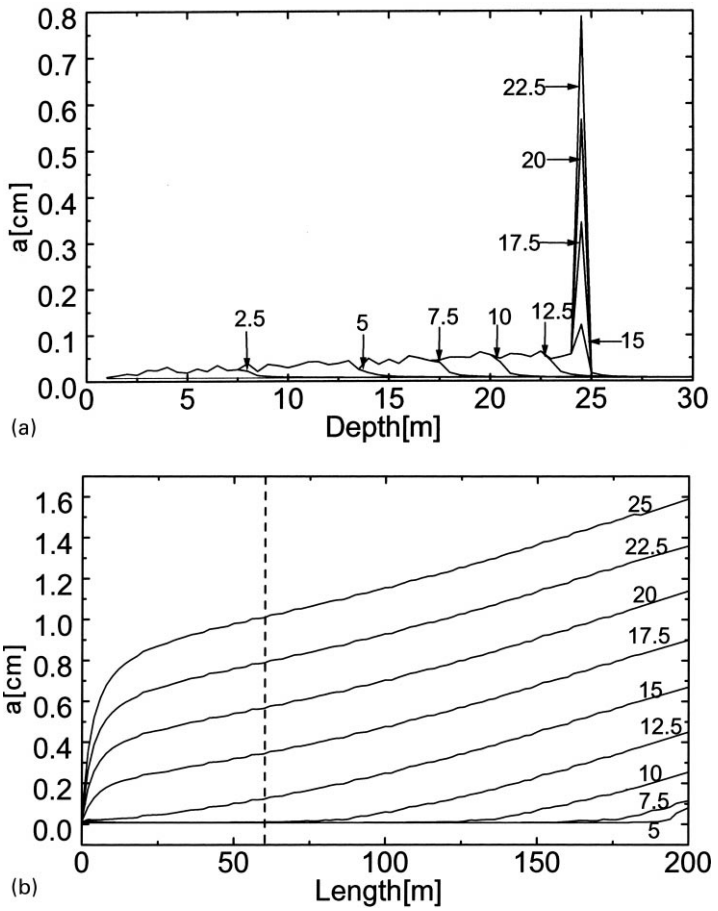

Fig. 3. (a) Profile of the widths of the horizontal fractures along a vertical cross-section marked by an arrow in Fig. 2c at various times. A front of increased permeability with fracture widths of several hundreds of a cm penetrates downward. This front is marked by an arrow. Numbers give the time in ky (kyears). (b) Evolution of the widths profile of the conduit at base level (cf. Fig. 2c and d) in time, given in ky by the numbers on the curves. Initial width is 7×10^{-3} cm. The conduit starts to grow headwards at 7.5 ky and shows a linear increase of its width in time. The dashed vertical line marks the position of the vertical profile shown in (a).

$k_4 = 4 \times 10^{-8}$ mol/(cm^2 s), $c_{eq} = 2 \times 10^{-6}$ mol/cm^3, $c_s = 0.9 c_{eq}$. We furthermore assume that before entering the water table, the concentration of the inflowing solution has reached $0.9 c_{eq}$ at all fractures, and that this value increases linearly with the depth of the water table to $0.97 c_{eq}$ at base level during all time steps of the model run. This accounts for the initial fast approach towards equilibrium, when the solution seeps through the soil and the vadose zone. As a consequence only fourth-order slow dissolution kinetics is active in the phreatic part of the aquifer.

Fig. 2a shows the water table after 50 years which is practically identical to the initial one. The phreatic zone is indicated by fat fracture lines, and the vadose zone by the thin lines. The colors show the fracture aperture width increasing from dark blue to red as denoted at the figure. At the permeable right-hand side of the cliff a seepage zone is established where flow seeps out from the fractures. Fig. 2b gives the position of the water table after 5000 years, which has dropped due to the increasing fracture widths in the aquifer. Fig. 2c shows the situation after 10 000 years, when the water table reaches the lowest possible output fractures. By continuous dissolution of these fractures a conduit develops, which grows headwards (Fig. 2d) until it reaches the left boundary after

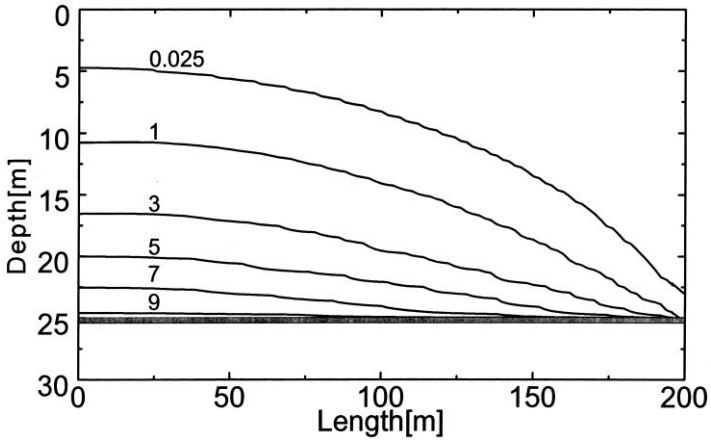

Fig. 4. Position of the water table at various times for an aquifer as in Fig. 2, but one prominent fracture with widths of 0.025 cm is added as indicated by the grey line. Number on the curves indicates time in ky.

20 000 years. Inspection of the colors in Fig. 2 reveals that the hydraulic conductivity increases by about 2 orders of magnitude leaving a highly permeable vadose zone as is observed in nature (cf. Eq. (2)).

Dissolutional widening is most active close to the water table at all times, since when penetrating into the net the solution approaches quickly towards equilibrium. Therefore close to the water table a narrow region of higher permeability is established where flow is concentrated. Fig. 2a presents a small light blue fringe indicating this. With increasing time the water table drops leaving behind the vadose region of increased conductivity. The phreatic zone below still has low hydraulic conductivity. In such an aquifer most of the flow is directed along the water table.

Fig. 2e depicts the dissolution rates after 5000 years (c.f. Fig. 2b), which are maximal close to the water table and drop significantly below. Fig. 2f shows the corresponding flow rates through the fractures and clearly illustrates (green, yellow, red fractures) that flow is restricted close to the water table.

As the water table drops, dissolution becomes active in the lower parts of the aquifer. Once the water table has reached a stationary position, dissolution stays active close to it and large conduits can grow. This corresponds to the ideal water table cave in the model of Rhoades and Sinacori (1941). A renewed lowering of the water table by incision of a valley will repeat this scenario until at the new level of the valley a lower water table cave starts to grow.

To illustrate the distribution of fracture widths in the net Fig. 3a shows the aperture widths of the horizontal fractures as a function of the distance from the top of the aquifer for various times. This distribution of fracture widths is taken along column 30 as indicated by an arrow in Fig. 2c. At time zero all fractures show the initial widths of 0.007 cm. Since dissolution occurs only close to the water table a region of widened fractures with an average width of about 0.03 cm propagates into the rock down to the position of the actual water table. This high permeability characterizes the vadose zone. Further dissolution by water trickling down this zone is not taken into account by our model. After 10 000 years the zone of widened fractures has dropped further until after 15 000 years the water table has reached the lowest horizontal fracture at the seepage face (cf. Fig. 2d). From then on this fracture widens continuously as depicted by the curves above 15 000 years. A similar behavior is also observed for the vertical fractures and is not shown here.

Fig. 3b shows the evolution of the horizontal fracture widths along the final water table. The spring is at the right-hand side. A conduit starts to grow headwards from the spring into the aquifer as soon as the water table has reached the spring. As the intersection of the water table and the horizontal fracture moves headwards the recharge is drained by the spring side part of the fracture, and the conduit widens at an almost constant rate. This explains the linear profiles.

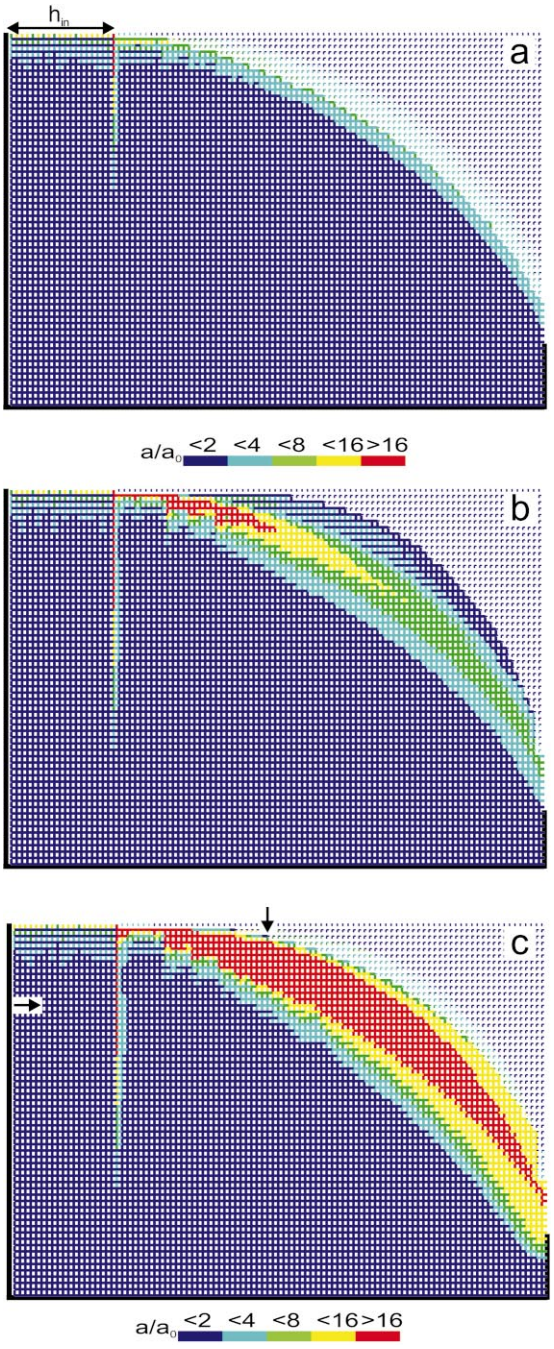

Fig. 5. Evolution of an aquifer with evenly spaced fractures as in Fig. 2, but constant head condition marked by an arrow in (a), and constant recharge else: The water table is fixed to the constant head region and dissolution is mainly active in a fringe close to it. (a) 1000, (b) 1750, (c) Breakthrough at 2100 years. At that time the widths of the fractures in the red area are about 0.2 cm.

Finally when the water table coincides with the entire fracture, we have the case of a one-dimensional conduit with evenly distributed recharge. This shows maximal rates at its end, which after a short distance level into a constant widening of about 0.1 cm/ky (kyears).

Our new concept of karst genesis shows that evolution of highly permeable aquifers including large conduits at the final position of the water table is possible also in the case of initially evenly fractured limestone without prominent fractures. Such prominent fractures were a necessary ingredient in both the models of Clemens et al. (1996) and those of Kaufmann and Braun (1999, 2000). Although these models deal with horizontally oriented cave systems, the physical and chemical processes active there are the same. In consequence one expects that their results should be comparable to ours. Without prominent fractures both models of Clemens and Kaufmann, respectively, should exhibit even widening of all fractures in the discrete fracture network. This should establish an even water table at their locations. In other words our one-dimensional final water table would be two-dimensional in their models.

It is well known in natural karst, however, that prominent bedding planes and joints exist along which caves can be guided (Ford and Williams, 1989). Knez (1997) showed that in the evolution of Skocjanske cave only three formative bedding planes were employed out of 62 observed. In a second scenario we have therefore included such a prominent bedding plane, with a width of 0.025 cm at base level into the aquifer. Fig. 4 indicates by a gray line the position of this fracture, which extends along the entire length of the aquifers. It further illustrates the position of the water table after various times. In comparison to Fig. 2a a significant drop of the initial water table below the surface of the aquifer is observed, since the prominent horizontal fracture receives vertical flow and conducts it to the exit. After 5000 years the water table has reached this fracture and at 10 000 years the water table coincides fully with it. The evolution of the aquifer generally is close to that in Fig. 2 but becomes faster. Therefore it is not shown in the figure. We have also modeled the case where a vertical fracture of 0.025 cm aperture width is added to this aquifer down all its depth at the position marked by arrows in Fig. 4. This does

not have significant influence to the evolution of the aquifer. The only difference is that increased width has been created along the fracture.

3.2. Homogenous aquifers: constant recharge and constant head conditions

In many cases of karst evolution constant head boundary conditions by a river or lake must be included. Fig. 5 shows such a case. We assume a constant head at the left upper boundary, equal to the elevation as indicated in the figure. Otherwise everything else is as in Fig. 2. Fig. 5a shows the water table and the distribution of fracture widths in the initial state. Due to the constant head condition the water table is tied to the region of constant head and cannot drop as in Fig. 2. Dissolution occurs only in a small banded region close to it. Therefore dissolutional widening remains restricted to this fringe as illustrated by Fig. 5a–c. Furthermore a dissolution channel develops vertically at the border between constant head and constant recharge conditions. With increasing time the regions of constant head and constant recharge are connected by high permeability fractures which attract additional flow from the constant head region. Therefore the water table rises as shown in Fig.5b (1750 years). After 2100 years (Fig. 5c) a banded zone of high conductivity has been created which carries increasing flow from the constant head area. Fig. 6 shows the total discharge as a function of time. This resembles a typical breakthrough behavior such as observed for one-dimensional conduits or for nets under constant head conditions. (Dreybrodt, 1996; Siemers and Dreybrodt, 1998). To obtain the same quantitative information on the widths of the fractures Fig. 7 exhibits the distribution of widths along a vertical and horizontal cross-section through the aquifer as indicated in Fig. 5c for various times.

If prominent fractures, connecting the region of constant head to the output are present the evolution of such fractures is close to evolution of a single tube under constant head. But there is also the evolution of a breakthrough behavior along the water table. A competition between these two pathways is to be expected. When the fractures are sufficiently wide, breakthrough time can be shorter than the time needed to create breakthrough along the water table. Such a situation is shown by Fig. 8, where a vertical and horizontal fissure of 0.03 cm aperture width connects the region of constant head to the spring. Everything else is as in Fig. 5. Fig. 8 illustrates the distribution of widths in a logarithmic scale at breakthrough of discharge through the prominent fracture after 300 years. The small fringe of enlarged fractures close to the water table indicates that evolution of this pathway needs much longer time (cf. Fig. 5). Fig. 9 depicts the width profiles of the single conduit along the prominent fracture for various times. After breakthrough constant recharge conditions must be

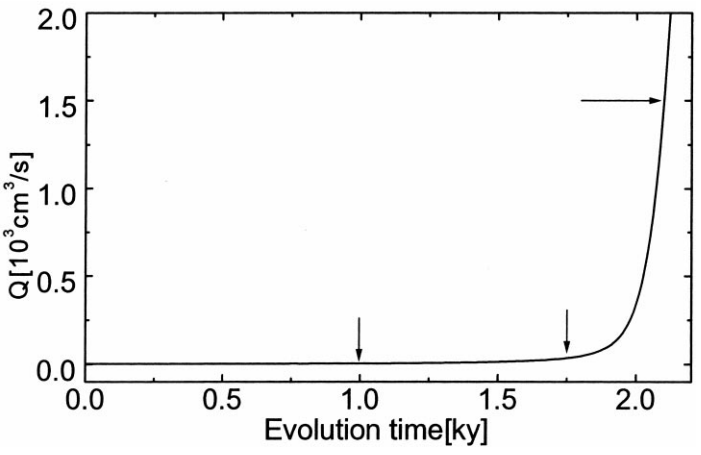

Fig. 6. Flow through the aquifer of Fig. 5 as a function of time. A typical breakthrough behavior is observed. The arrows indicate the times of Fig. 5a–c.

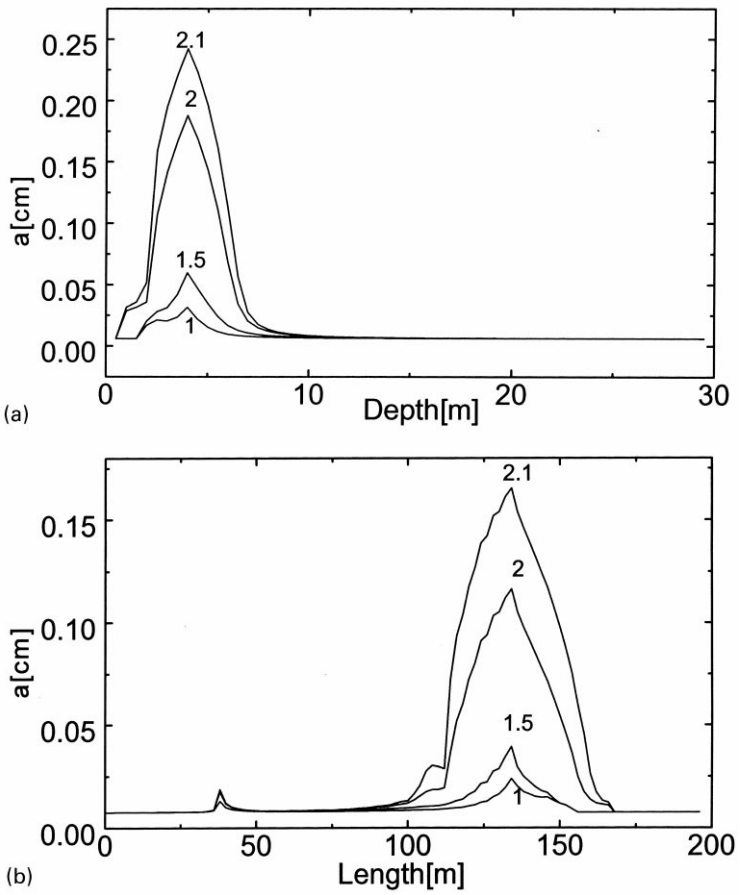

Fig. 7. Distribution of the fracture widths for the horizontal and vertical cross-section of the aquifer as indicted by the arrows in Fig. 5c. (a) Widths of the vertical fractures in the vertical cross-section for various times indicated in ky. The region of maximal widths corresponds to the red area in Fig. 5. (b) Widths of the horizontal fractures in the horizontal cross-section for various times. The small peak at about 30 m corresponds to the vertical channel which develops at the border between constant head and the constant recharge region.

assumed for the prominent fracture, draining all the recharge in the former area of constant head. Correspondingly the water table will decline similar as in Fig. 4 leaving a vadose zone of increased conductivity and further evolution of the conduit will be determined by constant recharge to it. This is not shown here.

3.3. Aquifers with a net of prominent fractures

A karst aquifer at its onset of evolution more realistically must be described by a superposition of at least two fracture networks. One is dense and evenly distributed, with fracture widths of several 10 μm, as it has been used in the examples of Figs. 2 and 5. The other one describes the wider prominent fractures. Such a network can be modeled by percolation methods as described by Siemers and Dreybrodt (1998). Fig. 10 shows the combination of these two fracture systems. The dense net is as in Fig. 2. To create the net of prominent fractures the following protocol is adopted. We divide the net of fine fractures into a coarse net of 5 by 5 dense fractures. Then by a method of random numbers to each of these longer horizontal or vertical fractures comprising this net, a width of 0.02 cm is assigned with a probability of $p = 0.7$. Otherwise the widths of the fracture is that of the dense net. By this way a coarse net of

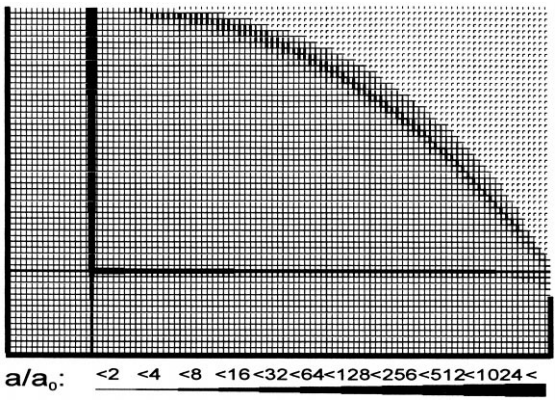

Fig. 8. Distribution of fracture widths at breakthrough for an aquifer as in Fig. 5, but with two additional prominent fractures with aperture width 0.03 cm connecting the region of constant head to the output at base level ($t = 300$ *years*).

statistically distributed prominent fractures is obtained. It should be noted, that all the parameters used in our model (Table 1) have clearly defined physical meaning, although they might not be to specify easily in a real karst system.

This initial scenario is similar to the approach of the model of Clemens et al. (1996) but it avoids the exchange coefficient, which is difficult to specify conceptually. It is also close to the approach of Kaufmann and Braun (1999, 2000) who model the initial aquifer by a superposition of a prominent fracture net to a rock matrix with homogenous initial conductivity. The most important difference in our approach is that dissolutional widening is regarded in both parts of the aquifer, whereas Clemens et al. and also Kaufmann and Braun disregard dissolution in the dense fractures or matrix, respectively.

The boundary conditions in the scenario of Fig. 10 are those of Fig. 5, constant head at the left-hand upper side and constant recharge else. Fig. 10a shows the widths at the onset of the evolution after 200 years. After 1000 years a complex net of conduits is seen along the prominent fractures (Fig. 10b). The region of constant head becomes connected to the area of constant recharge by increasing conductivity, caused by both widening of the fine fractures and also connection to the prominent ones. Consequently the water table rises. Close to the water table a region of higher conductivity connects the prominent fractures to the seepage face. This change of conductivity and hydraulic heads enhances the evolution of the conduits along the prominent fractures, which always proceeds along those pathways exhibiting highest hydraulic gradient and also the largest fracture widths. After 1200 years breakthrough occurs, with prominent fracture widths in the order of a few millimeters (Fig. 10c). To illustrate the distribution of fracture widths as they evolve in time Fig. 11 depicts these along a horizontal cross-section as indicated by an arrow in Fig. 10c. The discharge through the aquifer shows the characteristic breakthrough behavior. This event terminates early evolution of the model aquifer.

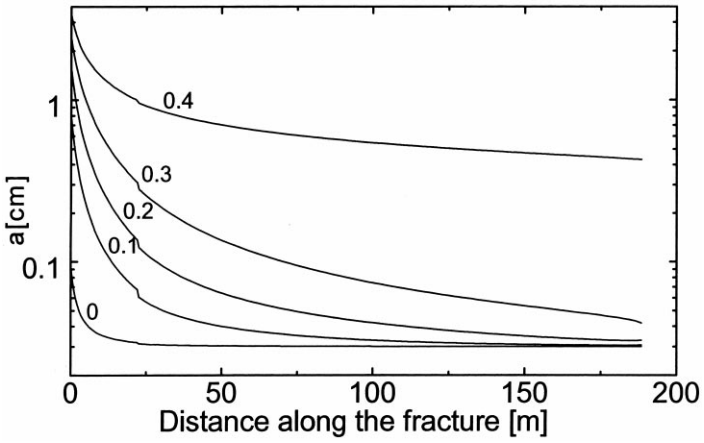

Fig. 9. Widths profile along the prominent fracture in the aquifer of Fig. 8 for various times indicated by the number on the curves (in ky). Input at 0 m, spring at 190 m.

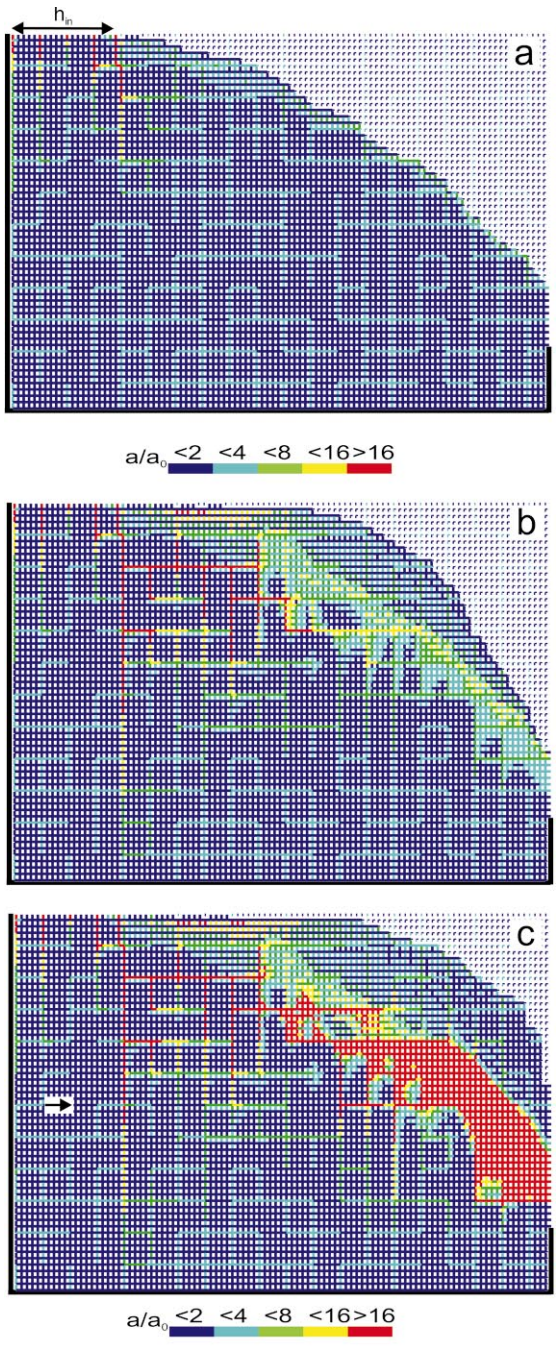

Fig. 10. Evolution of an aquifer with dense fractures as in Fig. 5, but with an additional percolation network of prominent fractures with aperture widths of 0.02 cm (light blue) for various times. (a) 200, (b) 1000, (c) 1200 years.

The constant head condition breaks down and must be replaced by constant recharge. Also flow will become turbulent. Nevertheless, the complicated pattern of vertical and horizontal conduits and the high permeability region close to the spring will be important for the future evolution of the mature karst aquifer, when by onset of turbulent flow heads are redistributed. It should be stressed at that point, that constant head conditions are crucial to the evolution of such complicated structures as shown in Fig. 10.

If however, boundary conditions of constant recharge are solely present, and also some prominent fractures exist an interesting competition becomes active which can also generate complex patterns. To elucidate this we start with a simple, idealized scenario. Fig. 12 shows the evolution of an aquifer with dense fractures identical to that of Fig. 2. But one pathway of a few prominent fractures with widths of 0.04 cm penetrates below base level and is terminated after the loop there. Initially the water table is high, as depicted by the dashed line in Fig. 12a, which illustrates the aquifer at 5000 years. It takes about 10 000 years until it has reached base level (Fig. 12b). During this time a hydraulic head acts along the prominent fracture and therefore it widens similarly as under constant head conditions from the input to the spring. Note that the dropping head is partially compensated by a reduced length of the fracture, since its upper part becomes vadose.

Fig. 13 shows the distribution of fracture aperture widths of the horizontal fractures along the cross-section containing the horizontal part of the prominent pathway in Fig. 12 as they evolve in time. The prominent horizontal fracture first widens slowly in time until 10 000 years, very similar as under constant head conditions. Breakthrough, however, is not accomplished. From then on its width increases linearly in time.

After 13 000 years a conduit has propagated at the base level headwards from the spring (Fig. 12c). At the left-hand side of the vertical fracture another conduit grows headwards also at the base level (Fig. 12c). Since the loop of the prominent fracture below base level has evolved to a width of about 3 mm this loop effectively drains water flowing along base level from the left-hand side. After about 15 000 years (not shown here) the entire flow is

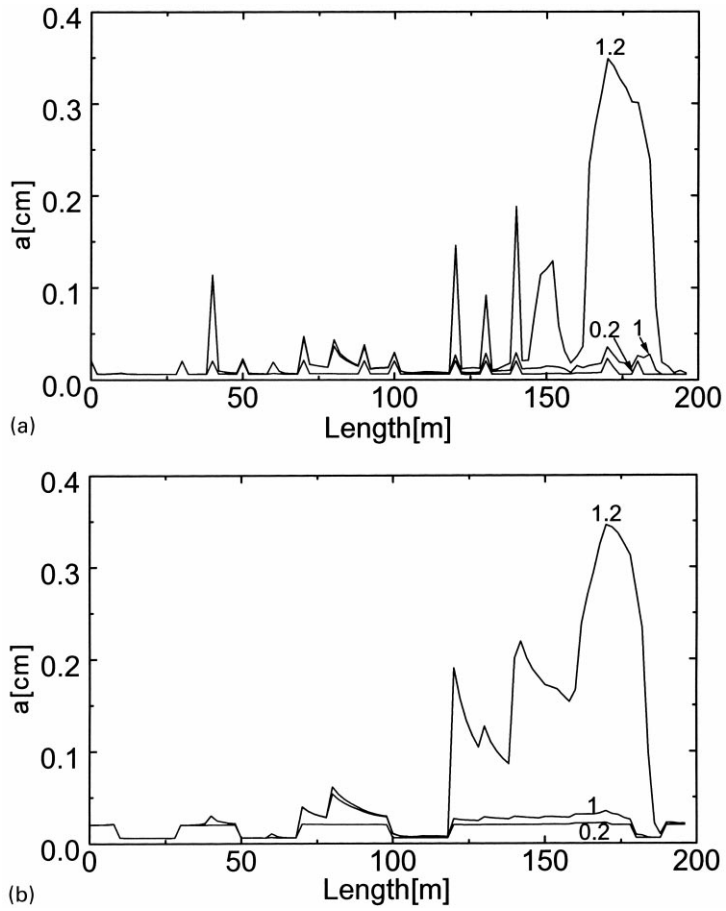

Fig. 11. (a) Profiles of horizontal fracture widths along a horizontal cross-section as marked by the arrow in Fig. 10c. (b) Profiles of vertical fracture widths along this cross-section. Times in ky are given by the numbers on the curves.

directed along the water table at the left side. From there it flows through the short circuiting loop and then again along the water table to the spring. A conduit then continues to grow along this stable flow path. Between the entrance and the exit of the loop at base level a watershed exists due to the left entrance of the loop which attracts flow from this region. Fig. 12d shows this situation at 3000 years.

If a percolation net of prominent fractures is present complex loops below base level can arise. This is shown by Fig. 14. It shows the aquifer with a network of prominent fractures ($p = 0.8$) with aperture widths of 0.04 cm. To get a more pronounced pattern, recharge is increased to 700 mm/year. Fig. 14a represents the fracture widths after 30 000 years. Fig. 14b depicts the flow rates and consequently the flow path at that time. These are the conduits which continue to grow below the water table as in Fig. 12, although here they are more complex.

4. Discussion and conclusion

We have presented a concept of karst aquifer evolution, using a superposition of two discrete networks. A dense one simulates the system of fine fractures, which in the model of Clemens would represent the continuum. These fractures after widening generate the later storage in the aquifer. A coarser net represents additional prominent fractures. Matrix permeability in this model has been neglected, which

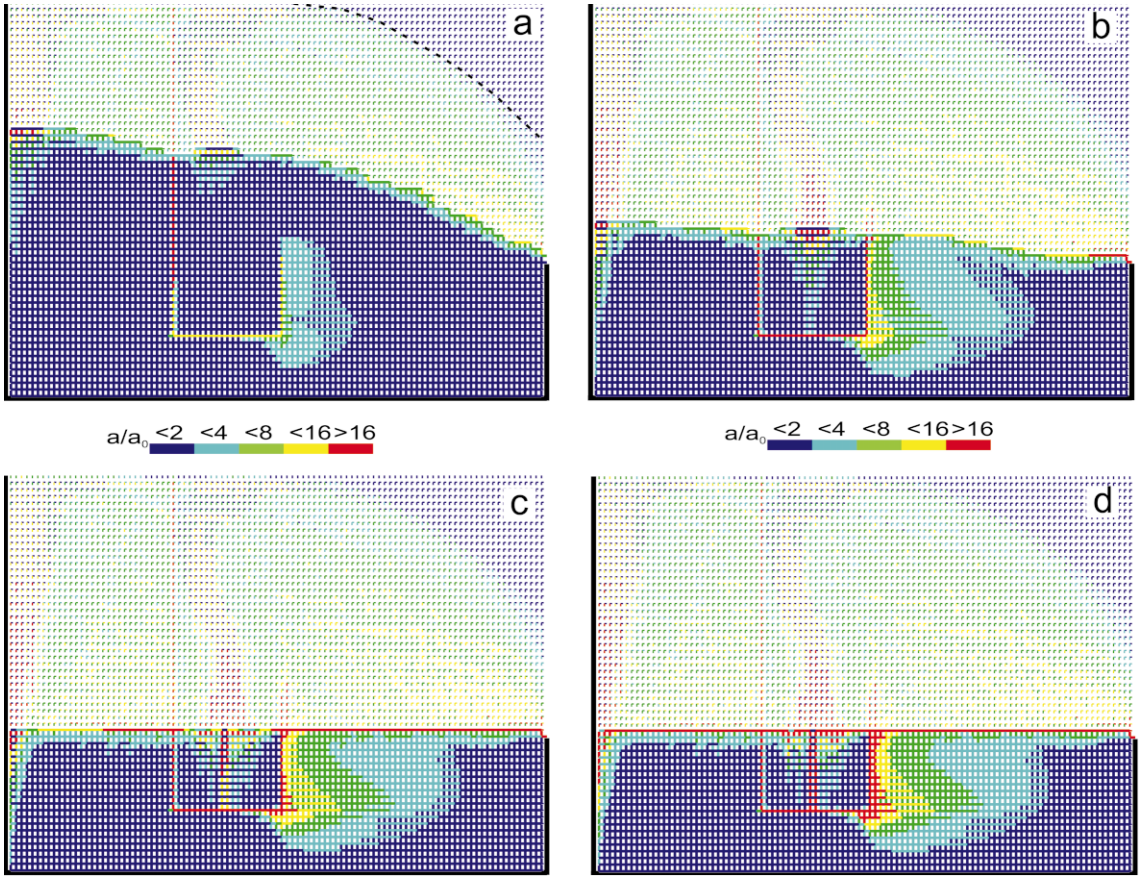

Fig. 12. Evolution of an aquifer with a pathway of prominent fractures ($a_p = 0.04$ cm). The dashed line in (a) depicts the initial water table. Distribution of fracture widths at (a) 5000, (b) 10 000, (c) 13 000, (d) 30 000 years, when all the flow from left is channeled through the loop of the prominent fracture below the water table.

is true for compact limestone, where the hydraulic conductivity is less than 10^{-10} ms^{-1}, (Halihan et al., 1999). The boundary conditions on the surface of the aquifer have been chosen as a combination of constant head and constant recharge. Consequently unconfined karst aquifers can be modeled, where due to dissolutional widening of the fractures in *both* fracture systems the position of the water table moves in time. Dissolution in the fracture system must be taken into account also to explain the evolution of storage in the network of the fine fractures. The initial porosity in the example of Fig. 2 is 1.25×10^{-4}. As one can see from Fig. 3 these fractures have been widened from 0.006 cm initial width to about 0.05 cm after 12 000 years. This yields a porosity of about 10^{-3}. Regarding, however, that dissolution in these fractures has been neglected in the vadose zone this value is too low. One might estimate roughly widening in the vadose zone by the down seeping water in the following way. We have assumed that, when water seeps through the vadose zone its concentration increases from $0.9c_{eq}$ at the upper input to $0.97c_{eq}$ at the water table. Assuming that widening is uniform in the vadose zone by mass balance one finds widening of 0.1 cm in 10 000 years. Thus a porosity of about 1% results after about 20 000 years. This number is not unrealistic.

It is also possible to simulate confined karst aquifers, by choosing suitable boundary conditions. Confined phreatic karst aquifers can exist only

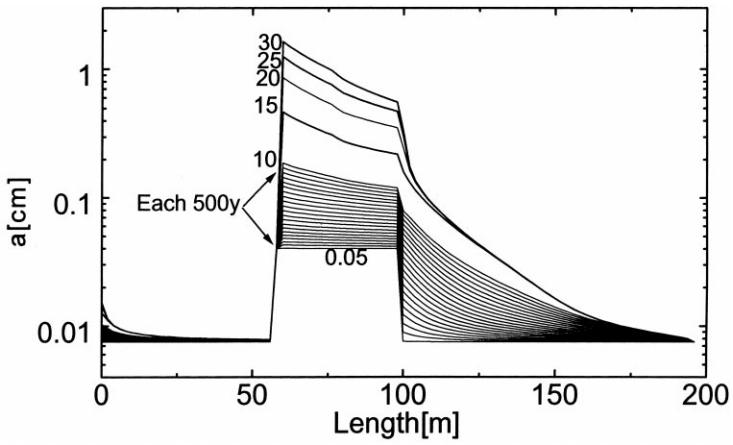

Fig. 13. Distribution of the horizontal fracture widths along the horizontal cross-section during the evolution of the aquifer. The cross-section contains the horizontal part of the prominent fracture between 60 and 100 m.

where the head in each location is higher than its local elevation above base level. This requires constant head conditions. The evolution of caves in such settings has been described from field evidence by Ford and Ewers (1978) and summarized by Ford and Williams (1989) and Ford (1999). They propose a four-state model of cave evolution, where in general dissolution conduits propagate from the input at higher elevation towards the spring. Single and multiple input scenarios have been suggested, to explain cave patterns. These scenarios have first been modeled by Ewers (1982), using hardware experiments. Bedding planes were constructed from plaster of Paris and a constant head was applied. In these experiments the evolution of protocaves toward the spring was observed in time scales of several days, until breakthrough occurred and the experiment was terminated (Ewers, 1978, 1982; Ewers and Quinlan 1981); see also Ford and Williams (1989) and Dreybrodt (1988). All scenarios proposed by Ewers were modeled recently by Dreybrodt and Siemers (2000) and showed the experimentally observed behavior. These confined aquifer models rely on the existence of prominent fractures connected from an input at constant head to the spring. They and the end members of our model are presented here.

A completely different model was proposed by Clemens et al. (1996, 1997, 1999). In this approach a single-continuum discrete-fracture model was used with constant recharge conditions. A continuum of fissures was assumed in the upper part of the aquifer. The system of prominent fractures (pipes) is located in a bedding plane at base level of the aquifer. Flow in the continuum was calculated by use of the computer program MODFLOW and coupled by an exchange term to the flow in the pipe system. By this way a two-dimensional model in width and length was obtained. Dissolutional widening was regarded exclusively in the prominent fractures, but not in the continuum of fine fractures overlying them.

Our model gives the evolution in depth and length. To compare this to the model of Clemens et al. we have replaced their two-dimensional plane with prominent fractures by one single fracture with 0.02 cm aperture width located at base level (cf. Figs. 2 and 4), and furthermore have assigned zero-dissolution rates to all the other fractures in the net. Therefore the concentration of the solution entering the water table equals that of the solution infiltrating at the top, where we assume $c = 0.95c_{eq}$. The general behavior of this model run is close to the one in Fig. 4 and is therefore not shown here. Due to the lower input concentration of $0.95c_{eq}$ (compared to that of $0.97c_{eq}$ in Fig. 4) into the lowest fracture the time needed for its evolution becomes shorter. This shows the importance to regard dissolution in the continuum. The concentration of the solution entering into the fracture determines critically the value of its dissolution rates. In our model the highest dissolution rates occur at the water table, where the solution

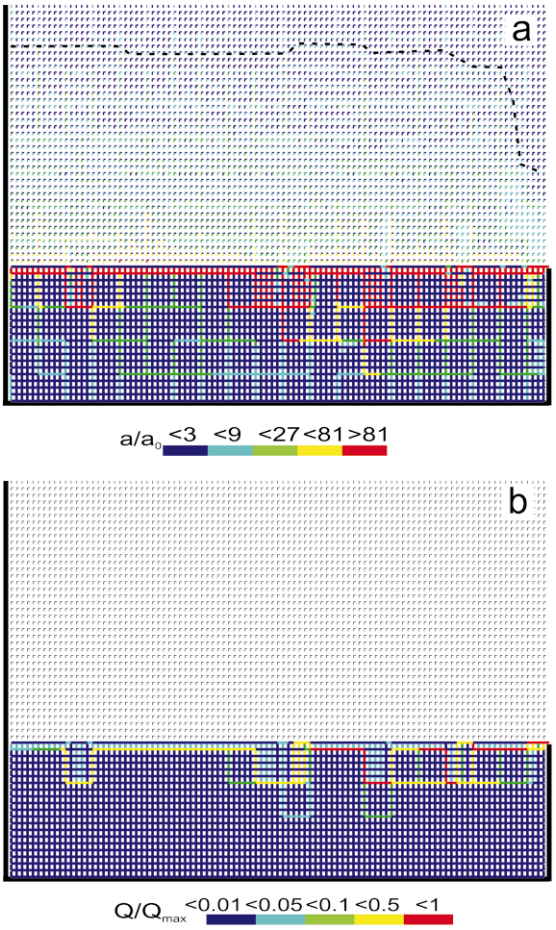

Fig. 14. Aquifer with a percolating net of prominent fractures (a_p = 0.04 cm). Annual precipitation is 700 mm/year. (a) Distribution of fracture widths after 30 000 years. Conduits grow along base level and phreatic loops. Note the change in the color code with respect to other figures. The widths designated by red are above 0.5 cm. The dashed line depicts the initial location of the water table. (b) Distribution of flow rates through the conduits depicted by the red conduits in (a).

enters directly into the fracture. They are significantly lower where the fracture is overlaid by the phreatic zone, because dissolution in this zone causes higher concentrations closer to equilibrium.

The comparison of these runs discussed above shows that our model at least conceptually contains the one of Clemens et al. (1996). It must be stated, however, that the hydrodynamic interaction between the flow systems in our model does not contain lateral flow, which can only be regarded by a three-dimensional model. The conduits evolving do also attract flow from the width of the aquifer. This is contained in the model of Clemens et al.

Our model goes beyond those proposed by Clemens et al. and Kaufmann and Braun. Its most important new features can be summarized by the following essentials, resulting from dissolutional widening in the system of dense narrow fractures.

1. Dissolutional widening is most active close to the actual water table and consequently a significant part of recharge is drained by the permeable fringe created there.
2. This mechanism causes lowering of the water table to its hydraulic lowest possible location, where dissolutional widening stays active, creating high permeability at this final water table.
3. If prominent fractures are present these, because of their low resistance to flow, guide phreatic loops below the final water table, and complex patterns of the distribution of hydraulic conductivities within the aquifer are created.

These principles are valid in any case of the architecture of the initial aquifer, for constant recharge or constant head conditions (cf. Figs. 2 and 4). One important consequence is that water table caves can originate under constant recharge conditions without the guidance by prominent fractures.

This resembles very close to older concepts of speleogenesis by Rhoades and Sinacori (1941), who proposed that dissolution occurs close to the actual water table in the epiphreatic zone. Therefore the water table should drop and the cave starts to develop, once the water table has reached base level. Cave development is therefore restricted to this region and conduits propagate headwards from the spring into the rock. These serve later as drainage of the water seeping through the vadose zone.

In the case of allogenic recharge by rivers constant head conditions can arise (cf. Figs. 5, 8 and 10). Therefore the water table is tied to this constant head region and remains restricted to a narrow region, where it can move as recharge increases due to increasing permeability close to the domain of constant head. Consequently increased permeability originates in a fringe almost

stable in time as long constant head conditions prevail (see Fig. 5). If no prominent fractures are present conduits can propagate from the input at constant head towards the spring. In this case the water table is fixed in space before any evolution of karst conduits has taken place. This scenario had been suggested by Swinnerton (1932). A short review of the models of Swinnerton, and Rhoades and Sinacori is given by Ford (1999). When additional prominent fractures are available as in Figs. 8 and 10 this water table concept breaks down, because a complex competition starts. Conduits start to grow under constant head conditions along the wide prominent fractures, and also in a fringe in the epiphreatic zone close to the water table. The increasing permeability of the latter can direct conduits growing along wide fractures towards the water table (cf. Fig. 10). Two extreme cases are possible, as illustrated by Figs. 5 and 8. If the breakthrough time for conduits propagating along prominent fractures is short compared to the time required for breakthrough along the water table fringe, complex conduit systems can originate in depth and length. As soon as breakthrough has occurred the constant head condition breaks down and the water table will drop to base level. On the other hand if breakthrough along the water table is effected first, a water table system is left. After breakthrough again constant recharge has to be assumed and the water table will drop towards base level.

Our model, although applicable in its present state only to cave evolution in depth and length, reconciles conflicting hypotheses and theories of cave genesis. It contains the four-state model (Ford, 1999; Ford and Williams, 1989) as well as the water table hypotheses by Swinnerton (1932) and Rhoades and Sinacori (1941). Which of those concepts is valid depends on the boundary conditions and the structure of the initial aquifer. Prominent fracture systems and constant head conditions favor evolution, which is well described by the four-state model by Ford and Ewers. Where initial porosity is sufficient for drainage of annual precipitation water table caves seem more likely. Constant recharge to karst plateaus favors the model of Rhoades and Sinacori.

Our model can also be used to describe early cave evolution under boundary conditions, changing in time. The simplest examples are tiered caves, which show cave passages in levels related to river terraces (White, 1988). These result from downcutting of valleys and can easily be treated with our model by lowering base level output.

Another scenario could be envisaged when a water table cave cuts into rock layers exhibiting significant prominent fractures. By some later event, as evolution of a vadose drawdown cave (Ford and Ewers, 1978) or downcutting of a valley, constant head conditions could arise which initiate a deep or shallow phreatic cave. Thus an aquifer can result which shows a water table cave in its upper part and a cave with phreatic loops below. Such a system is the Kolkbläser-Monster in the northern Austrian Alps (Steinernes Meer) as mapped by Denneborg (1997).

Our model does not contain dissolutional widening in the vadose zone. We have assumed furthermore that the recharge is evenly distributed to the actual water table. This is highly idealistic, since changes in the morphology of the surface and vadose widening can cause channeling of recharge to the actual water table. By this an interaction of the aquifer evolution and surface topography becomes active. This in principle can be incorporated in the future.

The model needs further extension. To simulate karst evolution in a larger scale from hundreds of meters in depth and thousand of meters in length much larger nets must be used. It is not simply possible to increase the size of the grids, the spacing of which represents the average distance between vertical joints or between bedding planes, respectively. To model larger karst systems the number of grids must be increased by about 10×10. The model presented here describes a comparatively small aquifer as could be imagined by a limestone quarry with a cliff of 30 m. The timescales until breakthrough will also depend on hydraulic head, infiltration rate, length of the aquifer and the initial aperture widths of the fractures. Sensitivity analysis should reveal this but is not the subject of this paper. Here we are interested in the conceptual results, which we believe, will be not affected in principle by changing these parameters. These detailed analysis will be done as soon as large karst aquifers in dimension of several hundred meters depth and a few kilometers length can be modeled by more

sophisticated programs. It also should be noted that a variety of boundary conditions, e.g. concentration of infiltration at some points at the surface, or varying lithology causing differing dissolution rates, could affect the results. Thus a variety of problems remains for future work.

The model calculations presented here have been performed on a relatively small aquifer with 30 m depth and 200 m length. But they are sufficient to illustrate qualitatively the mechanisms, which govern cave genesis in depth and length. A further shortcoming of this model is its restriction to length and depth.

If three-dimensional models become available it might be possible to design realistic models of actual karst regions, if sufficiently detailed knowledge of their structure is available. These could be used to investigate their hydrogeological properties, such as response of springs to recharge events or the distribution of pollutants injected at defined locations. Comparison to field evidence then can be used to understand in more detail what has to be regarded as a black box nowadays.

The aim of the work presented here is to show the feasibility of our approach and to initiate further research into this direction. Such work needs close cooperation of speleologists and hydrologists, who from field evidence are able to design realistic geological scenarios of karst aquifers and their history, and modelers, who can transform this geological knowledge into results, which can help to understand speleogenic processes.

Acknowledgements

Franci Gabrovšek thanks the University of Bremen for financial support. We thank A.N. Palmer and R. Liedl for their comments, which helped greatly to improve this work.

References

Buhmann, D., Dreybrodt, W., 1985. The kinetics of calcite dissolution and precipitation in geologically relevant situations of karst areas: 2. closed system. Chem. Geol. 53, 109–124.

Clemens, T., Hückinghaus, D., Sauter, M., Liedl, R., Teutsch, G., 1996. A combined continuum and discrete network reactive transport model for the simulation of karst development. Calibration and Reliability in Groundwater Modelling, IAHS Publication, vol. 237. IAHS, Colorado (pp. 309–318).

Clemens, T., Hückinghaus, D., Sauter, M., Liedl, R., Teutsch, G., 1997. Modelling the genesis of karst aquifer systems using a coupled reactive network model. Hard Rock Geosciences, IAHS Publication, vol. 241. IAHS, Colorado (pp. 3–10).

Clemens, T., Hückinghaus, D., Liedl, R., Sauter, M., 1999. Simulation of the development of karst aquifers: role of the epikarst. Int. J. Earth Sci. 88, 157–162.

Denneborg, M., 1997. Aufbau und Speleogenese eines hochalpinen Karstsystems (Kolkbläser-Monsterhöhle-System, Steineres Meer, Österreich; $L = 43$ m, HD $= -711$ m). Proceedings of the 12th International Congress of Speleology, vol. I, La Chaux-de-Fonds, Switzerland, pp. 341–344.

Dreybrodt, W., 1988. Processes in karst systems — physics, chemistry and geology. Springer Series in Physical Environments, vol. 5. Springer, Berlin, New York.

Dreybrodt, W., 1990. The role of dissolution kinetics in the development of karstification in limestone: a model simulation of karst evolution. J. Geol. 98, 639–655.

Dreybrodt, W., 1996. Principles of early development of karst conduits under natural and man-made conditions revealed by mathematical analysis of numerical models. Water Resour. Res. 32, 2923–2935.

Dreybrodt, W., Eisenlohr, L., 2000. Limestone dissolution rates in karst environments. In: Klimchouk, A., Ford, D.C., Palmer, A.N., Dreybrodt, W. (Eds.), Speleogenesis: Evolution of Karst Aquifers. Nat. Speleol. Soc., Huntsville, Alabama, USA.

Dreybrodt, W., Gabrovšek, F., 2000. Dynamics of the evolution of a single karst conduit. In: Klimchouk, A., Ford, D.C., Palmer, A.N., Dreybrodt, W. (Eds.), Speleogenesis: Evolution of Karst Aquifers. Nat. Speleol. Soc., Huntsville, Alabama, USA.

Dreybrodt, W., Lauckner, J., Zaihua, L., Svensson, U., Buhmann, D., 1996. The kinetics of the reaction $CO_2 + H_2O \rightarrow H^+ + HCO_3^-$ as one of the rate limiting steps for the dissolution of calcite in the system H_2–CO_2–$CaCO_3$. Geochim. Cosmochim. Acta 60, 3375–3381.

Dreybrodt, W., Siemers, J., 2000. Cave evolution on two-dimensional networks of primary fractures in limestone. In: Klimchouk, A., Ford, D.C., Palmer, A.N., Dreybrodt, W. (Eds.), Speleogenesis: Evolution of karst aquifers. Nat. Speleol. Soc., Huntsville, Alabama, USA.

Eisenlohr, L., Meteva, K., Gabrovšek, F., Dreybrodt, W., 1999. The inhibiting action of intrinsic impurities in natural calcium carbonate minerals to their dissolution kinetics in aqueous H_2O–CO_2 solutions. Geochim. Cosmochim. Acta 63, 989–1002.

Ewers, R.O., 1978. A model of the development of broad-scale networks of groundwater flow in steeply dipping carbonate aquifers. Trans. Cave Res. Group G. B. 5, 121–125.

Ewers, R.O., 1982. Cavern Development in the Dimensions of Length and Breadth. PhD thesis, McMaster University.

Ewers, R.O., Quinlan, J.F., 1981. Cavern porosity development in limestone: a low dip model for Mamoth Cave, KY. Proceedings of 8th International Congress of Speleology, Bowling Green, USA, pp. 721–731.

Ford, D.C., Ewers, R.O., 1978. The development of limestone caves

in the dimensions of length and depth. Can. J. Earth Sci. 15, 1783–1798.

Ford, D.C., Williams, P.W., 1989. Karst Geomorphology and Hydrology. Unwin Hyman, London.

Ford, D.C., 1999. Perspectives in karst hydrogeology and cavern genesis. In: Palmer, A.N., Palmer, M., Sasovsky, I.D. (Eds.). Karst Modeling. Karst Waters Institute, Charles Town, WV, pp. 17–29.

Ford, D.C., Lauritzen, S.E., Ewers, R.O., 2000. Hardware and software modeling of initial conduit development in karst rocks. In: Klimchouk, A., Ford, D.C., Palmer, A.N., Dreybrodt, W. (Eds.), Speleogenesis: Evolution of Karst Aquifers. Nat. Speleol. Soc., Huntsville, Alabama, USA.

Gabrovšek, F., Dreybrodt, W., 2000a. A model of early evolution of karst conduits affected by subterranean CO_2 sources. Environ. Geol. 39, 531–543.

Gabrovšek, F., Dreybrodt, W., 2000b. The role of mixing corrosion in calcite aggressive $H_2O–CO_2–CaCO_3$ solutions in the early evolution of karst aquifers. Water Resour. Res., 36, 1179–1188.

Groves, C.G., Howard, A.D., 1994a. Minimum hydrochemical conditions allowing limestone cave development. Water Resour. Res. 30, 607–615.

Groves, C.G., Howard, A.D., 1994b. Early development of karst systems.1. Preferential flow path enlargement under laminar flow. Water Resour. Res. 30, 2837–2846.

Halihan, T., Sharp, J.M., Mace, R.E., 1999. Interpreting flow using permeability at multiple scales. In: Palmer, A.N., Palmer, M., Sasovsky, I.D. (Eds.), Karst Modeling. Karst Waters Institute, Charles Town, WV, pp. 82–96.

Hanna, B.R., Rajaram, H., 1998. Influence of aperture variability on dissolutional growth of fissures in karst formations. Water Resour. Res. 34, 2843–2853.

Howard, A.D., Groves, C.G., 1995. Early development of karst systems 2. Turbulent flow. Water Resour. Res. 31, 19–26.

Kaufmann, G., Braun, J., 1999. Karst aquifer evolution in fractured, porous rocks. Water Resour. Res. 35, 3223–3238.

Kaufmann, G., Braun, J., 2000. Karst aquifer evolution in fractured rocks. Water Resour. Res. 36, 1381–1391.

Knez, M., 1997. Speleogenesis of phreatic channels in bedding-planes in the frame of karst aquifer (Skocjanske jame caves, Slovenia). Proceedings of 12th International Congress of Speleology, vol II. La Chaux-de-Fonds, Switzerland, pp. 279–282.

Lauritzen, S.E., Odling, N., Petersen, J., 1992. Modeling the evolution of channel networks in carbonate rocks. In: Hudson, J.A. (Ed.). ISRM Symposium: Eurock'92. Thomas Telford, London, pp. 57–62.

Lee, C., Farmer, I., 1993. Fluid Flow in Discontinuous Rocks. Chapman & Hall, London.

Palmer, A.N., 1984. Recent trends in karst geomorphology. J Geol. Educ. 32, 247–253.

Palmer, A.N., 1991. The origin and morphology of limestone caves. Geol. Soc. Am. Bull. 103, 1–21.

Palmer, A.N., 2000. Digital modeling of individual solution conduits. In: Klimchouk, A., Ford, D.C., Palmer, A.N., Dreybrodt, W. (Eds.), Speleogenesis: Evolution of karst aquifers. Nat. Speleol. Soc., Huntsville, Alabama, USA.

Plummer, L.N., Wigley, T.M.L., 1976. The dissolution of calcite in CO_2 saturated solutions at 25°C and 1 atmosphere total pressure. Geochim. Cosmochim. Acta 40, 191–202.

Rhoades, R., Sinacori, M.N., 1941. The pattern of ground-water flow and solution. J. Geol. 49, 785–794.

Sauter, M., 1991. Assessment of hydraulic conductivity in a karst aquifer at local and regional scale. Proceedings of Third Conference on Hydrogeology, Ecology, Monitoring and Management of Ground Water in Karst Terranes, Nashville, USA.

Sauter, M., 1993. Double porosity models in kartified limestone aquifers: field validation and data provision. In: Gültekin, G., Johnson, I.A. (Eds.), Hydrogeological Processes in Karst terraines. IAHS Publication, vol. 207. IAHS, Colorado, pp. 261–279.

Siemers, J., Dreybrodt, W., 1998. Early development of karst aquifers on percolation networks of fractures in limestone. Water Resour. Res. 34, 409–419.

Svensson, U., Dreybrodt, W., 1992. Dissolution kinetics of natural calcite minerals in CO_2–water systems approaching calcite equilibrium. Chem. Geol. 100, 129–145.

Swinnerton, A.C., 1932. Origin of limestone caverns. Geol. Soc. Am. Bull. 34, 662–693.

Teutsch, G., Sauter, M., 1991. Groundwater Modelling in karst terranes: scale effects, data acquisition and field validation. Proceedings of the Third Conference on Hydrogeology, Ecology, Monitoring and Management of Ground Water in Karst Terranes, Nashville, USA.

White, W.B., 1988. Geomorphology and Hydrology of Karst Terrains. Oxford University Press, New York.

Worthington, S.R.H., 1999. A comprehensive strategy for understanding flow in carbonate aquifers. In: Palmer, A.N., Palmer, M., Sasovsky, I.D. (Eds.), Karst Modeling. Karst Waters Institute, Charles Town, WV, pp. 17–29.

Worthington, S.R.H., Ford, D.C., 1997. Borehole tests for megascale channeling in carbonate aquifers. Proceedings of the 12th International Congress of Speleology, vol. 11, La Chaux-de-Fonds, Switzerland, pp. 195–198.